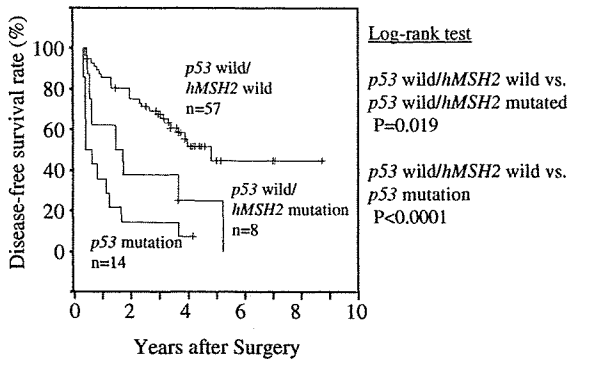

Fig. 1 – The Kaplan–Meier curves for disease-free survival for the three groups of HCC patients after a curative resection are shown: patients with *p53* mutation, those with *p53* wild/*hMSH2* mutation and those with *p53* wild/*hMSH2* wild.

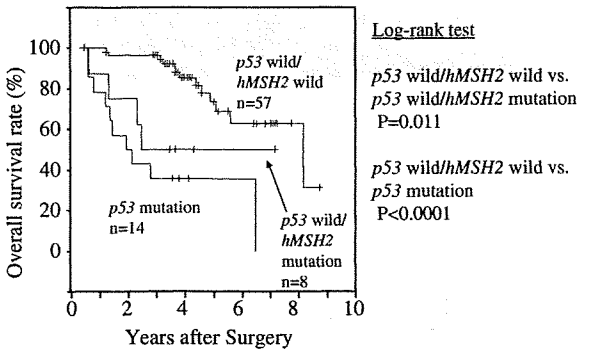

Fig. 2 – The Kaplan–Meier curves for overall survival for the three groups of HCC patients after a curative resection are shown: patients with *p53* mutation, those with *p53* wild/*hMSH2* mutation and those with *p53* wild/*hMSH2* wild.

Table 6 – The multivariate analysis of disease-free survival by means of the Cox's proportional hazard model

Variables		Risk ratio (95% CI)	P
Gene mutations	p53 wild/MSH2 wild	1 (reference)	
	p53 wild/MSH2 mutation	2.929 (1.241–6.915)	0.014
	p53 mutation	7.328 (3.470–15.474)	< 0.001
Liver cirrhosis	Negative	1 (reference)	
	Positive	2.106 (1.097–4.044)	0.025

with *p*53 and/or *h*MSH2 mutations in intrahepatic metastasis (75.0%) was significantly higher than that in multicentric occurrence (14.3%) ($P = 0.001$, respectively, Tukey's HSD test).

3.5. *Overall survival*

We also conducted univariate analysis for overall survival (OS) in all 79 HCC patients (Table 5). HCC patients with *p*53 mutation demonstrated a significantly shorter OS than those without (24 versus 98 months, $P < 0.0001$). In addition, liver cirrhosis also showed a significant difference ($P = 0.037$), while a marginal significance of OS was found for HCV status ($P = 0.068$).

We next analysed OS using only 65 HCC patients without *p*53 mutation as described above. Remarkably, HCC patients with *h*MSH2 mutation showed a significantly shorter OS compared with those without the mutation (30 versus 98 months, $P = 0.011$). Comparisons of OS among HCC patients with *p*53 mutation ($n = 14$), those with *p*53 wild/*h*MSH2 mutation ($n = 8$) and those without mutation ($n = 57$) are also shown in Fig. 2. The 3-year OS rates of HCC patients were 35.7%, 50.0% and 96.4%, respectively.

In the multivariate analysis, we included categories by *p*53 and *h*MSH2 mutation status, HCV and liver cirrhosis as explanatory variables that showed $P < 0.1$ in univariate analysis (Table 8). HCC patients with *p*53 wild/*h*MSH2 mutation and those with *p*53 mutation showed 6.8- and 14.5-fold risks compared with those without mutation ($P = 0.003$, $P < 0.001$, respectively). In addition, liver cirrhosis also revealed a statistically significant difference ($P < 0.001$). On the other hand, HCV did not show significance for OS in the analysis.

Table 7 – Recurrent pattern in HCC patients by status of *p*53 or *h*MSH2 mutation

		*p*53 and/or *h*MSH2 mutations	*p*53 wild/ *h*MSH2 wild	Frequency of mutated patients (%)	P
Recurrence	Intrahepatic recurrence				0.001*
	Intrahepatic metastasis (*n*)	12	4	75.0	0.001**
	Multicentric occurrence (*n*)	2	12	14.3	
	Unclassified (*n*)	1	4	20.0	
	Distant metastasis (*n*)	5	5	50.0	
	Total (*n*)	20	25	44.4	<0.001***
No recurrence		2	32	5.9	

* One way ANOVA for patients with intrahepatic recurrence.
** Tukey's HSD test for intrahepatic metastasis versus multicentric occurrence.
*** Fisher's exact test for recurrence versus no recurrence.

Table 8 – The multivariate analysis of overall survival by means of the Cox's proportional hazard model

Variable		Risk ratio (95% CI)	p
Gene mutations	p53 wild/MSH2 wild	1 (reference)	
	p53 wild/MSH2 mutation	6.813 (1.894–24.505)	0.003
	p53 mutation	14.504 (5.240–40.147)	0.001
Liver cirrhosis	Negative	1 (reference)	
	Positive	6.544 (2.298–18.637)	0.001
HCV	Negative	1 (reference)	
	Positive	3.060 (0.764–12.255)	0.11

4. Discussion

This study presents the results of an analysis of the clinical features of hepatocellular carcinoma in 83 HCC patients with and without *p53* and/or *hMSH2* mutations. Interestingly, HCC patients without mutations of these genes showed a better prognosis including recurrence and survival than those with gene mutations. Furthermore, *p53* or *hMSH2* mutation status was also found to be associated with the pattern of recurrence. These findings suggest that mutations of these genes may be deeply involved in not only the progression of HCC but also the recurrence development of HCC.

A *p53* or *hMSH2* gene mutation may accelerate the progressional development of HCC by a 100–600-fold increase in the rate of spontaneous mutations and accumulation due to defects in mismatch repair.[23,24] It is of course also possible that the loss of a mismatch repair function is likely to lead to high frequencies of ectopic recombination[25,26]; this may then lead to genomic rearrangement(s) and, as a result, activation of an oncogene or inactivation of a tumour suppressor gene, resulting in the acceleration of progression of HCC.

On the other hand, although *p53* or *hMSH2* mutation were not detected in non-malignant cells in cancer tissue, prognosis of the patients was worse than that without the mutations. This may be because the genome in normal cells around tumours is more instable in HCCs with *p53* or *hMSH2* mutation than those without these mutations, influencing the recurrence or survival. The possibility cannot be excluded that a few normal cells with *p53* or *hMSH2* mutation have existed within cancer tissue though we cannot detect these mutations by our assay system.

Cells in a tumour may well become resistant to chemotherapeutic agents following their acquisition of mutations that affect the *p53* or *hMSH2* genes[27–29]; this is because it should be much easier for cells that have a disrupted mismatch repair system to acquire a drug resistance phenotype by virtue of the increased mutability which stems from their genomic instability. Thus there may be significant differences in responsiveness to chemotherapy in HCC patients with *p53* and/or *hMSH2* mutations and without these mutations, and this could well lead to their experiencing significantly different survival periods following a relapse.

The recurrent tumours identified in this study were classified in accordance with the recommendations of the Liver Cancer Study Group of Japan in their paper on the classification of primary liver cancers.[30] Thus the term intrahepatic metastasis is used to describe: 1) tumours that can be clearly seen as having grown from portal vein tumour thrombi, 2) tumours that surround a large main tumour with multiple satellite nodules, and 3) a small solitary tumour which is close to the main tumour and is either histologically similar to or less differentiated than the main tumour. Multiple HCC lesions that cannot be described as metastases under the above criteria are believed to represent potential multicentric occurrences; such tumours are separately recorded as '*de novo carcinogenesis*'. However, there may often be recurrent tumours that are difficult to classify as either intrahepatic metastases or multicentric

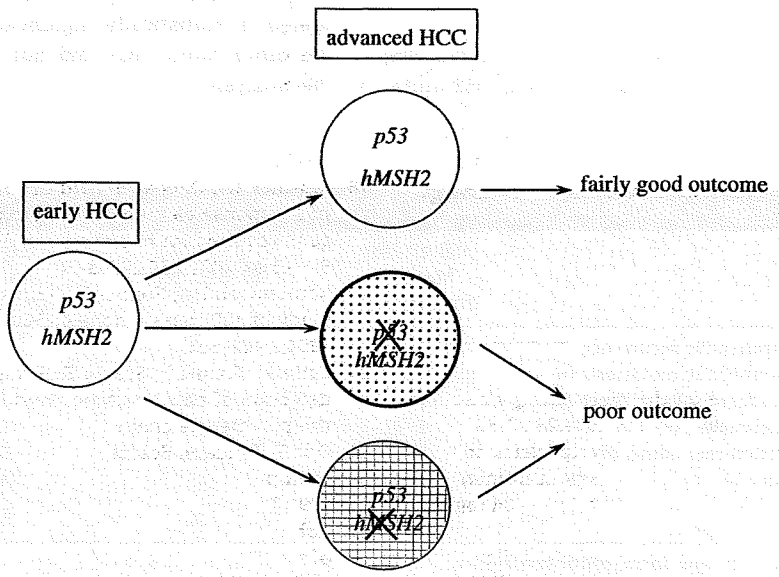

Fig. 3 – A proposed model of hepatocellular carcinogenesis with emphasis on progression in relation to mutations of p53 and *hMSH2* genes.

occurrences. Several studies have tried to examine the possible histologic[14] and genetic[31–33] differential diagnoses, but this is still impossible. In our present study, almost all of the cases in which we found a *p53* and/or an *hMSH2* gene mutation appeared to relapse within 2 years of surgery as a consequence of intrahepatic metastasis. Although we noted that the outcomes were reasonably good in the great majority of the *p53* wild/*hMSH2* wild cases, there were a few cases involving multicentric occurrence that led to relapses occurring 3-plus years after surgery. Frequency of multicentric occurrence was also higher in *p53* wild/*hMSH2* wild cases than in these mutation positive cases. These findings suggest that gene alterations other than mutations of *p53* and *hMSH2* may be involved in recurrence and survival. So, gene alterations, especially on DNA repair system including other mismatch repair genes, need to be analysed.

Fig. 3 summarises the situation as we found it in patients with HCC. There seemed to be relatively few mutations in either *p53* or *hMSH2* in early-stage HCCs. The early-stage HCCs then developed into advanced-stage HCCs, which were more than 2 cm in diameter and were either poorly or moderately de-differentiated. The outcome tended to be pretty poor in those HCC patients whose tumours showed clear evidence of *p53* or *hMSH2* mutations, whereas in patients whose tumours had no mutation of either gene the outcome tended to be somewhat better.

Conflict of interest statement

None declared.

Acknowledgement

The authors thank Dr. K. S. Iwamoto, UCLA, for discussions. We are also grateful to: Shiho Yano and Chiyoe Saitoh for excellent technical help.

This is part of a collaborative study between the liver disease projects of the Department of Surgery, Division of Frontier Medical Science, Graduate School of Biomedical Sciences, Hiroshima University and the Radiation Effects Research Foundation (RERF), Hiroshima, Japan. RERF is a private, nonprofit foundation funded equally by the Japanese Ministry of Health and Welfare and the U.S. Department of Energy through the National Academy of Sciences.

REFERENCES

1. Suriawinata A, Xu R. An update on the molecular genetics of hepatocellular carcinoma. *Semin Liver Dis* 2004;**24**:77–88.
2. Sun M, Eshleman JR, Ferrell LD, et al. An early lelsion in hepatic carcinogenesis: Loss of heterozygosity in human cirrhotic livers and dysplastic nodules at the 1p36-p34 region. *Hepatology* 2001;**33**:1415–24.
3. Yeh SH, Chen PJ, Shau WY, et al. Chromosomal allelic imbalance evolving from liver cirrhosis to hepatocellular carcinoma. *Gastroenterology* 2001;**121**:699–709.
4. Yano M, Asahara T, Dohi K, Mizuno T, Iwamoto KS, Seyama T. Close correlation between a *p53* or hMSH2 gene mutation in the tumor and survival of hepatocellular carcinoma patients. *Int J Oncol* 1999;**14**:447–51.
5. Katiya S, Dash BC, Thakur V, Guptan RC, Sarin SK, Das BC. P53 tumor suppressor gene mutations in hepatocellular carcinoma patients in India. *Cancer* 2000;**88**:1565–73.
6. Wang L, Bani-Hani A, Montoya D, et al. hMLH1 and hMSH2 expression in human hepatocellular carcinoma. *Int J Oncol* 2001;**19**:567–70.
7. Hussein MR. Alterations of p53, Bcl-2, and hMSH2 protein expression in the cirrhotic, macroregenerative, dysplastic nodules and hepatocellular carcinomas in upper Egypt. *Liver Int* 2004;**24**:552–60.
8. Salvucci M, Lemoine A, Saffroy R, et al. Microsatellite instability in European hepatocellular carcinoma. *Oncogene* 1999;**18**:181–7.
9. Macdonald GA, Greenson JK, Saito K, Cherian SP, Appelman HD, Boland CR. Microsatellite instability and loss of heterozygosity at DNA mismatch repair gene loci occurs during hepatic carcinogenesis. *Hepatology* 1998;**28**:90–7.
10. Zekri AR, Sabry GM, Bahnassy AA, Shalaby KA, Abdel-Wahabh S, Zakaria S. Mismatch repair genes (hMLH1, hPMS1, hPMS2, GTBP/hMSH6, hMSH2) in the pathogenesis of hepatocellular carcinoma. *World J Gastroenterol* 2005;**11**:3020–6.
11. Shimada M, Takenaka K, Gion T, et al. Prognosis of recurrent hepatocellular carcinoma: A 10-year surgical experience in Japan. *Gastroenterology* 1996;**111**:720–6.
12. Sugimachi K, Maehara S, Tanaka S, Shimada M, Sugimachi K. Repeat hepatectomy is the most useful treatment for recurrent hepatocellular carcinoma. *J Hepatobiliary Pancreat Surg* 2001;**8**:410–6.
13. Kumada T, Nakano S, Takeda I, et al. Patterns of recurrence after initial treatment in patients with small hepatocellular carcinoma. *Hepatology* 1997;**25**:87–92.
14. Shimada M, Hamatsu T, Yamashita Y, et al. Characteristics of multicentric hepatocellular carcinomas: Comparison with intrahepatic metastasis. *World J. Surg.* 2001;**25**:991–5.
15. Hussein MR, Hassan M, Wood GS. Morphological changes and apoptosis in radial growth phase melanoma cell lines following ultraviolet-B irradiation. *Am J Dermatopathol* 2003;**25**:466–72.
16. Karachristos A, Liloglou T, Field JK, Deligiorgi E, Kouskouni E, Spandidos DA. Microsatellite instability and *p53* mutations in hepatocellular carcinoma. *Mol Cell Biol Res Commun* 1999;**2**:155–61.
17. Scherer SJ, Welter C, Zang KD, Dooley S. Specific in vitro binding of p53 to the promoter region of the human mismatch repair gene hMSH2. *Biochem Biophys Res Commun* 1996;**221**:722–8.
18. Warnick CT, Dabbas B, Ford CD, Strait KA. Identification of a p53 response element in the promoter region of the hMSH2 gene required for expression in A2780 ovarian cancer cells. *J Biol Chem* 2001;**276**:27363–70.
19. Edmondson HA, Steiner PE. Primary carcinoma of the liver. A study of 100 cases among 48,900 necropsies. *Cancer* 1954;**7**:462–503.
20. Orita M, Suzuki Y, Sekiya T, Hayashi K. Rapid and sensitive detection of point mutation and DNA polymorphisms using the polymerase chain reaction. *Genomics* 1989;**5**:874–9.
21. Oda T, Tsuda H, Scarpa A, Skakmoto M, Hirohashi S. p53 gene mutation spectrum in hepatocellular carcinoma. *Cancer Res* 1992;**52**:6358–64.
22. Kobayashi K, Matsushima M, Koi S, et al. Mutational analysis of mismatch repair genes, hMLH1 and hMSH2, in sporadic endometrial carcinomas with microsatellite instability. *Jpn J Cancer Res* 1996;**87**:141–5.

23. Bhattacharyya NP, Skandalis A, Ganesh A, Groden J, Meuth M. Mutator phenotypes in human colorectal carcinoma cell lines. *Proc Natl Acad Sci USA* 1994;**91**:6319–23.
24. Hanford MG, Rushton BC, Gowen LC, Farber RA. Microsatellite mutation rates in cancer cell lines deficient or proficient in mismatch repair. *Oncogene* 1998;**16**:2389–93.
25. Wind N, Dekker M, Berns A, Radman M, Riele H. Inactivation of the mouse Msh2 gene results in mismatch repair deficiency, methylation torelance, hyperrecombination, and predisposition to cancer. *Cell* 1995;**82**:321–30.
26. Surtees JA, Argueso JL, Alani E. Mismatch repair proteins: key regulators of genetic recombination. *Cytogenet Genome Res* 2004;**107**:146–59.
27. Chan KT, Lung ML. Mutant p53 expression enhances drug resistance in a hepatocellular carcinoma cell line. *Cancer Chemother Pharmacol* 2004;**53**:519–26.
28. Rellecke P, Kuchelmeister K, Schachenmayr W, Schlegel J. Mismatch repair protein hMSH2 in primary drug resistance in in vitro human malignant gliomas. *J Neurosurg* 2004;**101**:653–8.
29. Lin X, Howell SB. DNA mismatch repair and p53 function are major determinants of the rate of development of cisplatin resistance. *Mol Cancer Ther* 2006;**5**:1239–47.
30. Liver Cancer Study Group of Japan. Classification of Primary Liver Cancer. Tokyo: Kanehara; 1997, p.38.
31. Yamamoto T, Kajino K, Kudo M, Sasaki Y, Arakawa Y, Hino O. Determination of the clonal origin of multiple human hepatocellular carcinomas by cloning and polymerase chain reaction of the integrated hepatitis B virus DNA. *Hepatology* 1999;**29**:1446–52.
32. Ng IO, Guan XY, Poon RT, Fan ST, Lee JM. Determination of the molecular relationship between multiple tumor nodules in hepatocellular carcinoma differentiates multicentric origin from intrahepatic metastasis. *J Pathol* 2003;**199**:345–53.
33. Morimoto O, Nagano H, Sakon M, et al. Diagnosis of intrahepatic metastasis and multicentric carcinogenesis by microsatellite loss of heterozygosity in patients with multiple and recurrent hepatocellular carcinomas. *J Hepatol* 2003;**39**:215–21.

Single nucleotide polymorphism in the *RAD18* gene and risk of colorectal cancer in the Japanese population

HIROTAKA KANZAKI[1], MAMORU OUCHIDA[1], HIROKO HANAFUSA[1], AKIKO SAKAI[1], HIROMASA YAMAMOTO[2], HIROMITSU SUZUKI[2], MASAAKI YANO[2], MOTOI AOE[2], KAZUE IMAI[3], HIROSHI DATE[2], KEI NAKACHI[3] and KENJI SHIMIZU[1]

[1]Department of Molecular Genetics and [2]Department of Cancer and Thoracic Surgery, Graduate School of Medicine, Dentistry and Pharmaceutical Sciences, Okayama University, Okayama 700-8558; [3]Department of Radiobiology/ Molecular Epidemiology, Radiation Effects Research Foundation, Hiroshima 732-0815, Japan

Received June 5, 2007; Accepted July 30, 2007

Abstract. The *RAD18* gene, located on the human chromosome 3p24-p25, plays a crucial role in post-replication repair (PRR) in various organisms from yeast to humans. In the human *RAD18* gene, one coding single nucleotide polymorphism (SNP) at codon 302, encoding either arginine (Arg, CGA) or glutamine (Gln, CAA), was reported. Although the molecular function of the RAD18 protein came to be elucidated, the association between the RAD18 Arg302Gln polymorphism and the risk of human cancer development was not examined. Therefore, we investigated the relationship between the polymorphism and the development of human primary colorectal cancer (CRC). The Arg302Gln polymorphism in 100 patients with CRC and 200 healthy controls were genotyped by the polymerase chain reaction with confronting two-pair primer (PCR-CTPP) assay. The Gln/Gln genotype was significantly more frequent in CRC (18.0%) than in the healthy controls (11.5%) (p=0.046). The increased risk was detected in CRC patients with the Gln/Gln genotype (Odds ratio [OR], 2.10; 95% confidence interval [CI], 1.00 to 4.40). When the relationship of the SNP with clinicopathological parameters of CRC was investigated, particularly in the well-differentiated grade and in the lymph node metastasis (N1) CRC patients, significantly higher risks were detected (OR, 7.00; 95% CI, 1.19-41.1 and OR, 3.71; 95% CI, 1.30-10.6, respectively). These results suggested that the RAD18 Arg302Gln polymorphism is associated with the risk of CRC. This report provides evidence for an association between the RAD18 Arg302Gln polymorphism and human CRC risk.

Correspondence to: Dr Mamoru Ouchida, Department of Molecular Genetics, Graduate School of Medicine, Dentistry and Pharmaceutical Sciences, Okayama University, 2-5-1 Shikata-cho, Okayama 700-8558, Japan
E-mail: ouchidam@md.okayama-u.ac.jp

Key words: single nucleotide polymorphism, RAD18, post-replication repair, colorectal cancer, cancer predisposition

Introduction

Any DNA damage induced by mutagens, such as UV light and mutagenic chemicals, must be repaired by DNA repair systems (1). However, when the DNA repair systems are stalled or saturated and such DNA damage is therefore not removed before the onset of DNA replication, single-stranded gaps are generated. These gaps will be filled by the post-replication repair (PRR) system. The molecular mechanisms of PRR are less clearly elucidated in comparison to the other repair pathways. The RAD6 pathway is known to be central to PRR (2). The genes belonging to the *RAD6* epistasis group, such as the *RAD5*, *RAD18*, *RAD30*, *MMS2* and *UBC13* genes, are all involved in the pathway. Among these gene products, RAD6 and RAD18 are two of the most important proteins and play a central role in this pathway. RAD6 is a ubiquitin-conjugating enzyme (E2) in the proteasome protein degradation system (3-5). RAD6 forms a tight complex with RAD18 (6-8), which is a single-strand DNA binding protein with a RING-finger domain (9) and ubiquitin-ligating enzymes (E3). Although RAD6 interacts with several E3, the interaction with RAD18 is essential for carrying out PRR (5,6,10,11). Since RAD6 interacts tightly with RAD18, although RAD6 does not have any DNA binding activity, it is proposed that RAD18 recruits RAD6 to the site of DNA damage via its physical interaction, where RAD6 and its complex then modulate stalled DNA replication through their ubiquitin-conjugating activity. There are reports that the proliferating cell nuclear antigen (PCNA), a DNA polymerase sliding clamp that is involved in DNA synthesis and repair, is a substrate of the ubiquitin-conjugating enzyme and it is ubiquitinated in a RAD6- and RAD18-dependent manner. Therefore, the monoubiquitination of PCNA through RAD6 and RAD18 is necessary for carrying out DNA PRR (12-16).

It was also reported that RAD18 knockout cells of mouse embryonic stem cells (17) and of chicken DT40 cells (18) were hypersensitive to various DNA-damaging agents and showed

defective PRR. These cells also showed genomic instability demonstrated by increased rates of the sister chromatid exchange and integration of the exogenous DNA (17,18). Therefore, the dysfunction of RAD18 increases the frequency of homologous recombination and illegitimate recombination and RAD18 contributes to the maintenance of genomic stability through PRR (19). The dysfunction of RAD18 is also thought to lead to the development of cancer (1,20).

The genetic polymorphisms of DNA repair genes were analyzed to determine the susceptibility to several cancers, including lung (21,22), colorectal (23), head and neck (24), breast (25), bladder cancer (26) and leukemia (27). The *RAD18* gene is known to have a single nucleotide polymorphism (SNP) at codon 302, encoding either arginine (CGA) or glutamine (CAA), while the function of this SNP and its molecular mechanism is not clarified. We conducted a pilot study to see whether the RAD18 Arg302Gln polymorphism is associated with cancer-incidence and found a significant correlation with CRC. This report provides evidence for an association between the RAD18 Arg302Gln polymorphism and human CRC risk.

Table I. Characteristics of CRC patients and healthy controls.

	Patients n (%) (n=100)	Controls n (%) (n=200)	p-value
Gender			0.371
Male	61 (61.0)	133 (66.5)	
Female	39 (39.0)	67 (33.5)	
Age (years ± SD)	65.1±10.1	65.6±9.42	
Smoking habit			0.052[a]
No-smoker	42 (42.0)	63 (31.5)	
Smoker	55 (55.0)	137 (68.5)	
<20 pack-years	14 (25.5)	17 (12.4)	
≥20 pack-years	40 (72.7)	87 (63.5)	
Unknown	1 (1.8)	33 (24.1)	
Unknown	3 (3.0)	0 (0.0)	

The mean age of each group with a standard deviation is shown. [a]p-values are for the differences in the number of smokers and non-smokers between the patients and the controls.

Materials and methods

Subjects. We analyzed 100 Japanese patients chosen from those who were histologically diagnosed as having primary colorectal cancer and who underwent surgical operation at Okayama University Hospital (Okayama, Japan) in 1994-2003. Patients were gathered not only from Okayama but also from 10 other prefectures in Western Japan, mainly the Chugoku and Shikoku Districts (around Okayama). We confirmed that all CRC patients have primary colorectal carcinomas by microscope. Clinical stage and pathological grade in all CRC patients were confirmed by operation and pathology. The clinicopathological staging and histological classification were according to the criteria of the UICC Tumor-Node-Metastasis Classification of Malignant Tumor (TNM), 6th edition, 2002, colon and rectum (ICD-O C18-C20). For the controls, each of the 200 healthy controls we analyzed were selected by computer-aided randomization, all of which were from the subjects of cohort studies on a Japanese general population >40 years of age in a town near the Saitama Cancer Center. The residents in this town are neither genetically nor demographically close, *i.e.*, its population increased because of a population influx from other areas, with a social increase rate of about 5% every year for 15 years. Written informed consent was obtained from all of the cancer patients and controls concerned. This study was approved by The Bioethics Committee of Okayama University Medical School. The characteristics of the 100 CRC patients and the 200 controls are shown in Table I. There were no significant differences in gender and age at recruitment between the CRC patients and the controls ($p \geq 0.05$). Pack-year equivalents [(cigarettes/day/20) x (smoking years)] were used for smoking status (we could not obtain smoking status for 3 out of the 100 patients).

DNA extraction. The genomic DNA of cancer patients was isolated from the non-cancerous region of the resected specimens or from the mononuclear cells of the peripheral blood by the standard method of proteinase K digestion and phenolchloroform extraction. The genomic DNA of the healthy controls was extracted from the peripheral lymphocytes.

Genetic analysis. The RAD18 Arg302Gln polymorphism was detected by polymerase chain reaction using the confronting two-pair primer (PCR-CTPP) method (28,29). According to the published sequence of the human *RAD18* gene, we designed two sets of paired primers. The first set of primers was as follows: forward primer 1, 5'-ATA CCC ATC ACC CAT CTT C-3' and reverse primer 1, 5'-GTC TTC TCT ATA TTT TCG ATT TCT T-3' for the Gln allele amplifying a 146-bp band. The second set of primers was as follows: forward primer 2, 5'-TTA ACA GCT GCT GAA ATA GTT CG-3' and reverse primer 2, 5'-CTG AAA TAG CCC ATT AAC ATA CA-3' for the Arg allele amplifying a 106-bp band. A 206-bp band was designed between the forward primer 1 and the reverse primer 2. The reaction mixture (20 μl) contained 40 μM of each dNTP, 1X PCR buffer, 8 pmol of the forward primer 1 and reverse primer 2, 24 pmol of the forward primer 2 and reverse primer 1, 20 ng of the genomic DNA and 0.5 units of the Taq DNA polymerase (Takara, Kyoto, Japan). The PCR amplification was initiated by a denaturing step at 94°C for 3 min, followed by 35 cycles at 94°C for 30 sec, 64°C for 1 min, 72°C for 1 min and a final extension step at 72°C for 7 min. For genotyping, the PCR products were subjected to electrophoresis in 3% agarose gel, stained with ethidium bromide and then visualized on a UV transilluminator. In order to confirm the allele types, certain PCR products were processed with the Big Dye terminator Cycle Sequencing Kit (Applied Biosystems, Foster City, CA, USA), then analyzed and confirmed on an ABI 3100 sequencer (Applied Biosystems).

Statistical analysis. We compared the allele frequencies of the Arg/Gln (CGA/CAA) polymorphism in the *RAD18* gene between the healthy control group and the patient groups with

CRC. The distribution of the *RAD18* genotype (Arg/Arg, Arg/Gln, Gln/Gln) in all of the patients and the controls was tested for adherence to the Hardy-Weinberg equilibrium. The statistical analyses were conducted by the SPSS software Ver.12.0 (SPSS Inc., Tokyo, Japan). The Chi-square test was used to compare the genotype distribution between the cancer patients and the healthy controls. The odds ratio (OR) and 95% confidence interval (95% CI) were both adjusted for age, gender and smoking status using an unconditional logistic regression model. The relationship between the genotype and the clinicopathological parameters was examined by the Chi-square test and Fisher's exact probability test. A p-value of <0.05 was considered to be statistically significant.

Results

Assessment of cancer risk by RAD18 genotyping. The characteristics of the 100 CRC patients and the 200 healthy controls are shown in Table I. There were no significant differences in gender, age or smoking status between the two groups. Pack-year equivalents were used for smoking status (however, we could not obtain the smoking status for 3 out of the 100 CRC patients).

Fig. 1A shows a representative polymerase chain reaction with confronting two pair primer (PCR-CTPP) assay patterns of the Arg/Gln (CGA/CAA) genotypes in the codon 302 of the RAD18 gene. The allele types were determined as follows: two fragments of 205- and 106-bp for the Arg/Arg (G/G) genotype, two fragments of 205- and 146-bp for the Gln/Gln (A/A) genotype and three fragments of 205-, 146- and 106-bp for the Arg/Gln (G/A) genotype. We confirmed that each PCR mixture contained no non-specific bands by electrophoresis in 3% agarose gel. The genotypes were confirmed by the subsequent sequencing of representative cases (Fig. 1B).

The genotype analysis of this SNP revealed that the genotype frequency was significantly different between the control and patient groups. The frequencies of the three genotypes in the *RAD18* gene are shown in Table II. The frequencies of the genotypes Arg/Arg, Arg/Gln and Gln/Gln found were 43.0, 45.5 and 11.5% in the controls and 32.0, 50.0 and 18.0% in the CRC patients. All of the results fitted the Hardy-Weinberg equilibrium. Compared to the controls with

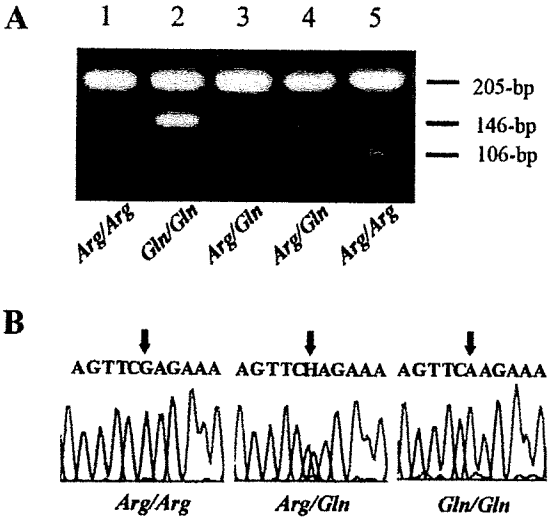

Figure 1. The single nucleotide polymorphism of the *RAD18* gene at codon 302. (A) The PCR-CTPP patterns of the *RAD18* SNP. The PCR product was electrophoresed in 3% agarose gel. Two fragments of 205- and 106-bp show the Arg/Arg (G/G) genotype, two fragments of 205- and 146-bp show the Gln/Gln (A/A) genotype and three fragments of 205-, 146- and 106-bp show the Arg/Gln (G/A) genotype. The case number and genotypes are shown at the top and bottom, respectively. (B) DNA sequence patterns of the *RAD18* SNP. Heterozygous signals (G/A) are shown by arrows in the Arg/Gln genotype.

the Arg/Arg genotype, CRC patients with the homozygous Gln/Gln genotype exhibited the most significantly increased risk with an odds ratio (OR) of 2.10 (95%CI, 1.00-4.40), therefore suggesting that the homozygous Gln/Gln (A/A) genotype has an enhanced risk of CRC development.

The association between the RAD18 genotype and clinicopathological parameters in CRC patients. When we analyzed the relationship between the genotype distribution and the clinicopathological parameters of the CRC patient group, the well-differentiated grade and lymph node metastasis (N1) patients with the A/A genotype exhibited a significantly increased risk with an adjusted OR of 7.00 (95% CI=1.19-41.1) and 3.71 (95%CI=1.30-10.6), respectively (Table III). There were no overall differences in genotype distribution within each parameter using the Chi-square test or the

Table II. The RAD18 genotypes in CRC patients and healthy controls.

RAD18 genotype	Patients n (%)	Controls n (%)	p-value	OR (95% CI)
Arg/Arg	32 (32.0)	86 (43.0)		Ref. 1
Arg/Gln	50 (50.0)	91 (45.5)	0.151[a]	1.47 (0.87-2.52)
Gln/Gln	18 (18.0)	23 (11.5)	0.046[a]	2.10 (1.00-4.40)
Total	100	200		
Allele frequencies			0.037	
Arg	114 (57.0)	263 (67.8)		
Gln	86 (43.0)	137 (34.2)		

[a]p-values are shown against Arg/Arg genotype between patients and controls.

Table III. Association between the RAD18 genotype and clinicopathological parameters of CRC patients.

Characteristics	Genotype (%)				p-value[a]	OR[b] (95%CI)	
	Arg/Arg	Arg/Gln	Gln/Gln	Total		Arg/Gln	Gln/Gln
Differentiated grade					0.172		
Well	2 (11.1)	11 (61.1)	5 (27.8)	18		4.71 (1.00-22.2)	7.00 (1.19-41.1)
Moderate	25 (33.8)	36 (48.6)	13 (17.6)	74		1.31 (0.72-2.39)	1.68 (0.72-3.89)
Poor	2 (66.7)	1 (33.3)	0 (0.0)	3		NE	NE
Others	3 (60.0)	2 (40.0)	0 (0.0)	5			
T					0.007		
Tis, T1, T2	0 (0.0)	10 (71.4)	4 (28.6)	14		NE	NE
T3, T4	32 (37.2)	40 (46.5)	14 (16.3)	86		1.14 (0.65-2.00)	1.32 (0.58-3.00)
N					0.097		
N0	13 (28.9)	24 (53.3)	8 (17.8)	45		1.55 (0.73-3.31)	1.82 (0.63-5.18)
N1	9 (25.0)	18 (50.0)	9 (25.0)	36		1.91 (0.81-4.51)	3.71 (1.30-10.6)
N2	9 (56.3)	7 (43.7)	0 (0.0)	16		0.75 (0.27-2.10)	NE
Unknown	1 (33.3)	1 (33.3)	1 (33.3)	3			
M					0.622		
M0	20 (29.9)	34 (50.7)	13 (19.4)	67		1.59 (0.84-3.01)	2.22 (0.93-5.33)
M1	12 (38.7)	15 (48.4)	4 (12.9)	31		1.18 (0.52-2.70)	1.19 (0.35-4.10)
Unknown	0 (0.0)	1 (50.0)	1 (50.0)	2			
TNM stage					0.929		
0.I.II	12 (30.8)	20 (51.3)	7 (17.9)	39		1.47 (0.66-3.26)	1.66 (0.55-5.02)
III.IV	20 (34.5)	28 (48.3)	10 (17.2)	58		1.35 (0.71-2.60)	1.84 (0.75-4.53)
Unknown	0 (0.0)	2 (66.7)	1 (33.3)	3			

[a]p-values were calculated by the Chi-square test or the Fisher's exact test. [b]ORs were adjusted for age, gender and smoking status. The Arg/Arg genotype was defined as the reference. T, primary tumor; N, lymph node metastasis; M, distant metastasis; NE, not estimated.

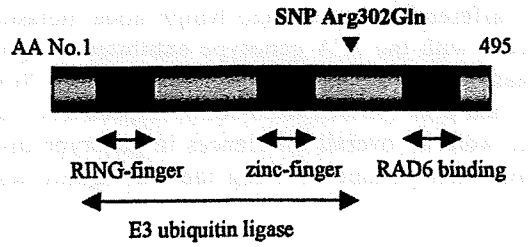

Figure 2. The location of the polymorphism and the functional motifs of RAD18. The SNP (Arg302Gln) is indicated by an arrowhead above the motif. The motifs of the RAD18 protein are depicted in dark gray and/or by arrows. The RING-finger, a really interesting new gene domain (AA25-63); zinc-finger, zinc-finger motif (AA201-223); RAD6 binding, RAD6 binding domain (AA371-410); E3 ubiquitin ligase, RING-finger-containing E3 ubiquitin-ligase domain (AA16-304). AA No., amino acid number.

Fisher's exact test, while the genotype distribution in the tumor stages may be biased due to the small sample size.

Discussion

In this study, we examined whether an SNP (Arg302Gln) in the *RAD18* gene is associated with the risk for the development, progression and metastasis of CRC. We found significant differences in the genotype distribution between the CRC patients and the healthy controls. Our findings suggest that the Gln allele enhance the susceptibility to the development of CRC (p=0.046, OR=2.10). We also found a significant association between polymorphism and clinicopathological features, specifically in differentiated grade and lymph node metastasis. The Gln allele was detected more frequently in patients with well-differentiated grade and lymph node metastasis (N1) (OR=7.00 and 3.71, respectively). These data also suggest that this SNP may become a prognostic marker. Our findings suggest an association between the RAD18 Arg302Gln polymorphism and the risk of CRC. No other studies have found any association between human cancers and the RAD18 SNPs.

Although the molecular mechanism of the association between this SNP and cancer development is not yet clarified, several of the functions and functional domains of RAD18 were revealed. RAD18 is one of the most important proteins involved in the PRR pathway. While a number of proteins are known to be involved in the PRR pathway and RAD18 interacts with several of these proteins, the interaction with RAD6 in particular is essential for carrying out PRR (5,6,10,11). RAD18 interacts with RAD6 through the RAD6 binding domain in the C-terminal region (Fig. 2). RAD18 has several other functional domains, such as the RING-finger

motif (25), zinc-finger motif (30,31) and E3 ubiquitin-ligase domain. The RING-finger motif, residing in the N-terminal region and the E3 ubiquitin-ligase domain together confer an ubiquitin-ligase activity on RAD18. The middle part of RAD18 contains a zinc-finger motif, which is considered to mediate protein-to-protein interaction or DNA binding. The RAD18 Arg302Gln polymorphism is located in the E3 ubiquitin-ligase domain (Fig. 2). Therefore, this SNP may affect the activity of RAD18, especially the ubiquitin-ligase activity. It is also possible that this SNP may affect the interaction between RAD18 and other proteins involved in PRR through its structural change, which is generated by the substitution of one amino acid residue, a basic amino acid residue (Arg), to a neutral residue (Gln). Considering that the Gln/Gln genotype was much more frequently found in the CRC patients than in the controls, the RAD18 with the Gln genotype may have decreased PRR activity and consequently may affect cancer development and progression.

In conclusion, our data provide evidence for an association between the RAD18 Arg302Gln polymorphism and the risk for the development and progression of CRC. It is possible that this polymorphism may influence susceptibility to a variety of human cancers through incomplete PRR. Further study with sufficiently larger populations and functional analysis of this polymorphism is needed in order to clarify this issue. Although the sample size we analyzed was small, the findings of this study are statistically significant. We expect that this study may contribute to the development of a novel strategy for the early diagnosis and prevention of CRC.

Acknowledgements

We thank the members of our University Hospital for their cooperation in specimen-sampling. This study was supported by a Grant-in-Aid for Scientific Research on Priority Area (No.12213084) to KS from the Ministry of Education, Culture, Sports, Science and Technology of Japan.

References

1. Hoeijmakers JH: Genome maintenance mechanisms for preventing cancer. Nature 411: 366-374, 2001.
2. Lawrence C: The RAD6 DNA repair pathway in Saccharomyces cerevisiae: what does it do, and how does it do it? Bioessays 16: 253-258, 1994.
3. Sung P, Prakash S and Prakash L: Mutation of cysteine-88 in the Saccharomyces cerevisiae RAD6 protein abolishes its ubiquitin-conjugating activity and its various biological functions. Proc Natl Acad Sci USA 87: 2695-2699, 1990.
4. Sung P, Prakash S and Prakash L: Stable ester conjugate between the Saccharomyces cerevisiae RAD6 protein and ubiquitin has no biological activity. J Mol Biol 221: 745-749, 1991.
5. Wood A, Schneider J, Dover J, Johnston M and Shilatifard A: The Paf1 complex is essential for histone monoubiquitination by the Rad6-Bre1 complex, which signals for histone methylation by COMPASS and Dot1p. J Biol Chem 278: 34739-34742, 2003.
6. Bailly V, Lamb J, Sunq P, Prakash S and Prakash L: Specific complex formation between yeast RAD6 and RAD18 proteins: a potential mechanism for targeting RAD6 ubiquitin-conjugating activity to DNA damage sites. Genes Dev 8: 811-820, 1994.
7. Bailly V, Lauder S, Prakash S and Prakash L: Yeast DNA repair proteins Rad6 and Rad18 form a heterodimer that has ubiquitin-conjugating, DNA binding and ATP hydrolytic activities. J Biol Chem 272: 23360-23365, 1997.
8. Bailly V, Prakash S and Prakash L: Domains required for dimerization of yeast Rad6 ubiquitin-conjugating enzyme and Rad18 DNA binding protein. Mol Cell Biol 17: 4536-4543, 1997.
9. Joazeiro CA and Weissman AM: RING-finger proteins: mediators of ubiquitin-ligase activity. Cell 102: 549-552, 2000.
10. Dohmen RJ, Madura K, Bartel B and Varshavsky A: The N-end rule is mediated by the UBC2 (RAD6) ubiquitin-conjugating enzyme. Proc Natl Acad Sci USA 88: 7351-7355, 1991.
11. Sung P, Berleth E, Pickart C, Prakash S and Prakash L: Yeast RAD6 encoded ubiquitin conjugating enzyme mediates protein degradation dependent on the N-end-recognizing E3 enzyme. EMBO J 10: 2187-2193, 1991.
12. Haracska L, Torres-Ramos CA, Johnson RE, Prakash S and Prakash L: Opposing effects of ubiquitin conjugation and SUMO modification of PCNA on replicational bypass of DNA lesions in Saccharomyces cerevisiae. Mol Cell Biol 24: 4267-4274, 2004.
13. Hoege C, Pfander B, Moldovan GL, Pyrowolakis G and Jentsch S: RAD6-dependent DNA repair is linked to modification of PCNA by ubiquitin and SUMO. Nature 419: 135-141, 2002.
14. Stelter P and Ulrich HD: Control of spontaneous and damage-induced mutagenesis by SUMO and ubiquitin conjugation. Nature 425: 188-191, 2003.
15. Kannouche PL, Wing J and Lehmann AR: Interaction of human DNA polymerase eta with monoubiquitinated PCNA: a possible mechanism for the polymerase switch in response to DNA damage. Mol Cell 14: 491-500, 2004.
16. Watanabe K, Tateishi S, Kawasuji M, Tsurimoto T, Inoue H and Yamaizumi M: Rad18 guides poleta to replication stalling sites through physical interaction and PCNA monoubiquitination. EMBO J 23: 3886-3896, 2004.
17. Tateishi S, Niwa H, Miyazaki J, Fujimoto S, Inoue H and Yamaizumi M: Enhanced genomic instability and defective post-replication repair in RAD18 knockout mouse embryonic stem cells. Mol Cell Biol 23: 474-481, 2003.
18. Yamashita YM, Okada T, Matsusaka T, *et al*: RAD18 and RAD54 cooperatively contribute to maintenance of genomic stability in vertebrate cells. EMBO J 21: 5558-5566, 2002.
19. Shekhar MP, Lyakhovich A, Visscher DW, Heng H and Kondrat N: Rad6 overexpression induces multinucleation, centrosome amplification, abnormal mitosis, aneuploidy and transformation. Cancer Res 62: 2115-2124, 2002.
20. Friedberg EC: DNA damage and repair. Nature 421: 436-440, 2003.
21. Ryk C, Kumar R, Thirumaran RK and Hou SM: Polymorphisms in the DNA repair genes XRCC1, APEX1, XRCC3 and NBS1 and the risk for lung cancer in never- and ever-smokers. Lung Cancer 54: 285-292, 2006.
22. Ito H, Matsuo K, Hamajima N, *et al*: Gene-environment interactions between the smoking habit and polymorphisms in the DNA repair genes, APE1 Asp148Glu and XRCC1 Arg399Gln, in Japanese lung cancer risk. Carcinogenesis 25: 1395-1401, 2004.
23. Yamamoto H, Hanafusa H, Ouchida M, *et al*: Single nucleotide polymorphisms in the EXO1 gene and the risk of colorectal cancer in a Japanese population. Carcinogenesis 26: 411-416, 2005.
24. Huang WY, Olshan AF, Schwartz SM, *et al*: Selected genetic polymorphisms in MGMT, XRCC1, XPD and XRCC3 and risk of head and neck cancer: a pooled analysis. Cancer Epidemiol Biomarkers Prev 14: 1747-1753, 2005.
25. Costa S, Pinto D, Pereira D, *et al*: DNA repair polymorphisms may contribute differentially on familial and sporadic breast cancer susceptibility: a study on a Portuguese population. Breast Cancer Res Treat 103: 209-217, 2007.
26. Zhu Y, Lai M, Yang H *et al*: Genotypes, haplotypes and diplotypes of XPC and risk of bladder cancer. Carcinogenesis 28: 698-703, 2007.
27. Bolufer P, Barragan E, Collado M, Cervera J, López JA and Sanz MA: Influence of genetic polymorphisms on the risk of developing leukemia and on disease progression. Leuk Res 30: 1471-1491, 2006.
28. Hamajima N: PCR-CTPP: a new genotyping technique in the era of genetic epidemiology. Expert Rev Mol Diagn 1: 119-123, 2001.
29. Hamajima N, Saito T, Matsuo K, Kozaki K, Takahashi T and Tajima K: Polymerase chain reaction with confronting two-pair primers for polymorphism genotyping. Jpn J Cancer Res 91: 865-868, 2000.
30. Mackay JP and Crossley M: Zinc fingers are sticking together. Trends Biochem Sci 23: 1-4, 1998.
31. Akhtar A and Becker PB: The histone H4 acetyltransferase MOF uses a C2HC zinc finger for substrate recognition. EMBO Rep 2: 113-118, 2001.

Available online at www.sciencedirect.com
ScienceDirect
Mutation Research 631 (2007) 55–61
Genetic Toxicology and Environmental Mutagenesis
www.elsevier.com/locate/gentox
Community address: www.elsevier.com/locate/mutres

High-throughput spectrophotometric assay of reactive oxygen species in serum

Ikue Hayashi [a], Yukari Morishita [b], Kazue Imai [b], Masakazu Nakamura [c], Kei Nakachi [b], Tomonori Hayashi [b,*]

[a] *Central Research Laboratory, Hiroshima University Faculty of Dentistry, 1-2-3 Kasumi, Minami Ward, Hiroshima 734-8553, Japan*
[b] *Department of Radiobiology/Molecular Epidemiology, Radiation Effects Research Foundation, 5-2 Hijiyama Park, Minami Ward, Hiroshima 732-0815, Japan*
[c] *Department of Health Promotion and Education, Osaka Medical Center for Health Science and Promotion, 1-3-2 Nakamichi, Higashinari-ku, Osaka 537-0025, Japan*

Received 4 January 2007; received in revised form 9 April 2007; accepted 14 April 2007
Available online 20 April 2007

Abstract

The derivatives of reactive oxygen metabolites (D-ROM) test has been developed to determine the amount of oxygen-centered free radicals in a blood sample as a marker of oxidative stress. This study aims to improve the D-ROM test and develop an automated assay system by use of a clinical chemistry analyzer. Five microliters of serum was added to 1 well of a 96-well microtiter plate for a total 240 μl of reaction solution containing alkylamine and metals. This was followed by automatic mixing, incubation and measurement of reactive oxygen species (ROS) levels as a color development at 505 nm using a spectrophotometer with catalytic capability for transition metals. This assay system was used to measure serum levels of ROS in cigarette smokers and never-smokers, by way of example. The levels of serum ROS determined by this system correlate with the amounts of free radicals and peroxides, which reacted with various molecules in the body and formed stable metabolites. This test can use frozen sera as well as fresh ones. The inter- and intra-deviation of this system was within 5% and showed consistent linearity in the range between 4 and 500 mg/l of hydrogen peroxides. Serum ROS levels among smokers increased with the number of cigarettes smoked per day (36.5% increment per pack per day; $P < 0.0001$). This assay system will be a simple, inexpensive, and reliable tool for assessing oxidative stress in human populations. Our preliminary results on cigarette smoking imply that this assay system has potential for application in various epidemiological and clinical settings.

Keywords: Reactive oxygen species; Reactive oxygen metabolites; Free radical; Smoking

1. Introduction

There is increasing concern about the deleterious effects that endogenously produced free radicals (i.e., reactive oxygen species, ROS, and nitrogen oxides) may exert on health. Excessive production of free radicals, specifically ROS, has been reported to have an association with a wide variety of clinical disorders, including cardiovascular disease, diabetes, and cancer [1–3]. ROS is produced in normal biological processes in the cells by means of either enzymatic or non-enzymatic mechanisms. Biologically relevant ROS include superoxide radical anion ($O_2^{\bullet -}$), hydroxyl radicals ($^{\bullet}OH$), hydro-

* Corresponding author. Tel.: +81 82 261 3131; fax: +81 82 261 3710.
E-mail address: tomo@rerf.or.jp (T. Hayashi).

1383-5718/$ – see front matter © 2007 Elsevier B.V. All rights reserved.
doi:10.1016/j.mrgentox.2007.04.006

gen peroxide (H_2O_2), alkoxy radicals ($RO^•$), and peroxy radicals ($ROO^•$), as well as singlet oxygen ($^1O_2^-$). It is widely accepted that ROS play both beneficial and adverse roles in an organism.

Free radicals are highly reactive molecules with a very short half-life. They can be measured directly by an electron spin resonance (ESR) spectrometer [4], or indirectly by an ESR spectrometer coupled with a spin-trapping method [5–8]. However, the technique of ESR spectroscopy requires extremely intricate and costly instruments. For these reasons, a simple method was recently developed to determine serum ROS levels: the derivatives of reactive oxygen metabolites (D-ROM) test [9], which is now recognized as an efficient method for evaluating oxidative stress in the body [10–15]. It has been reported that serum ROS levels in patients with ROS-related diseases, such as cancer, cardiovascular disease, and diabetes are higher than those in healthy people [16–18]. The microplate assay system was also developed for measurement of oxidative stress levels in pigs and birds [19–21]. However, these systems still need to be improved for routine measurements of ROS levels in a large number of serum samples at clinical laboratories. Precise measurement of ROS levels requires a series of complicated procedures that are often difficult to achieve at laboratories, especially when measuring a large number of samples. On the basis of the principle of the D-ROM test, we have developed an improved assay system that allows high-throughput and automated analysis of numerous serum samples with high reproducibility, consistent accuracy, and much smaller amounts of sera and reagents than with the conventional D-ROM test.

The reaction of this system:

$$R\text{–}OOH + Fe^{2+} \rightarrow R\text{–}O^• + Fe^{3+} + OH^- \text{ or}$$

$$R\text{–}OOH + Fe^{3+} \rightarrow R\text{–}OO^• + Fe^{2+} + H^+ \text{ or}$$

$$R\text{–}O^• + [Fe{=}O]^{2+} + H^+.$$

$$R\text{–}O^• \text{ or } R\text{–}OO^• + A\text{–}NH_2 \rightarrow R\text{–}O^- \text{ or } R\text{–}OO^- + [A\text{–}NH_2^•]^+ \text{ (coloured)}$$

R–OOH, $R\text{–}O^•$, $R\text{–}OO^•$, and $A\text{–}NH_2$ are generic peroxide, the alkoxyl radical of a generic peroxide, the peroxyl radical of a generic peroxide, and *N,N*-diethyl-*para*-phenylendiamine (chromogenic substrate), respectively. $[A\text{–}NH_2^•]^+$ is the coloured radical cation of the chromogenic substrate.

In this paper, the usefulness of the new assay system is demonstrated by assessing the effects of cigarette smoking on oxidative status in terms of serum ROS levels.

2. Materials and methods

2.1. Reagents

N,N-diethyl-*para*-phenylendiamine (DEPPD) sulfate and ferrous sulfate were purchased from Sigma Chemicals (St. Louis, MO, USA). Hydrogen peroxide was obtained from Wako Chemicals (Osaka, Japan). All other chemicals were commercially available. DEPPD was dissolved in 0.1 M sodium acetate buffer (pH 4.8) to attain a final concentration of 100 μg/ml (R_1 solution as a chromogen), and ferrous sulfate was dissolved in 0.1 M sodium acetate buffer (pH 4.8) to attain a final concentration of 4.37 μM (R_2 solution as a transition-metal ion). Hydrogen peroxide solution, attenuated to specified concentrations, was used as standard solution for generating a calibration curve. To process the reaction, 96-well microtiter plates (Nalge Nunc International, USA) were used. The Spectra Max Plus (Molecular Device Corp., USA) was used as a spectrophotometric plate reader.

2.2. Total ROS assay system with 96-well microtiter plate

Five microliters of either hydrogen peroxide standard solution (for generating a calibration curve) or serum was added to 140 μl of 0.1 M sodium acetate buffer (pH 4.8) in 1 well of a 96-well microtiter plate, which reached a temperature of 37 °C after 5 min. One hundred microliters of the mixed solution, which was prepared from R_1 and R_2 at a ratio of 1:25 before use, was added to each well as a starter. Then, after pre-incubation at 37 °C for 1 min using a spectrophotometric plate reader, absorbance at 505 nm was measured for a fixed time (between 60 and 180 s) at 15-s intervals. A calibration curve was automatically constructed from the slopes, which were calculated based on varying (delta) absorbance at 505 nm each time (min) corresponding to the concentration of hydrogen peroxide. ROS levels in serum were calculated by the analyzer (spectrophotometric plate reader) from the calibration curve, and expressed as equivalent to levels of hydrogen peroxide (1 unit = 1.0 mg H_2O_2/l).

The serum ROS levels determined by this assay system were compared with those measured by the conventional D-ROM test, using the FRAS 3 (IRAM SRL, Italy). In brief, 20 μl serum and 1.2 ml buffered solution (R_2 reagent) were mixed in a cuvette, and 20 μl chromogen substrate (R_1 reagent) was added to the cuvette. After shaking to mix, the cuvette was centrifuged for 1 min at 37 °C and incubated for 5 min at 37 °C. Absorbance increase at 505 nm was monitored for 3 min.

2.3. Subjects

This study examined serum ROS levels in a total of 252 healthy male workers. Of them, 212 subjects were current smokers who were participating in a stop smoking program conducted by Osaka Cancer Prevention and Detection Center in Osaka, Japan, in 1997–2000 [22]. All subjects were free from relevant inflammation-related diseases, such as myocar-

dial infarction and infectious diseases, which are the greatest confounding factors to study the effect of cigarette smoking on ROS levels. Their sera were collected at the time of entering the program (before intervention); age ranged from 20 to 60 years (mean ± S.D., 37.9 ± 10.1 years), and numbers of smokers by cigarette consumption were 35, 86, 56, and 35 for <20, 20–29, 30–39, and ≥50 cigarettes per day, respectively. Forty male never-smokers as in-house controls were recruited from the staff of Saitama Cancer Center Research Institute and Radiation Effects Research Foundation. All subjects gave informed consent for use of their serum samples. All samples were unlinkably anonymized and stored at −80 °C.

2.4. Statistics

The two-tailed independent-samples *t*-test was used in comparing serum ROS levels of smoker and never-smoker groups: differences in ROS levels were considered to be significant at $P < 0.05$. We examined the association between serum ROS levels and daily cigarette consumption using ANOVA of univariate, and we assessed the effects of cigarette smoking and aging on serum ROS levels by linear regression analysis based on the log of ROS level, adjusting for age and cigarette consumption. "SPSS for Windows" program (version 11.5) was used for statistical analyses.

3. Results

In 1 well (5 μl serum) of a 96-well microtiter plate, instead of the cuvette (20 μl serum, 1.2 ml R_2 reagent, and 20 μl R_1 reagent) used in the conventional D-ROM test, the reaction was automatically processed and monitored using a spectrophotometric plate reader. Absorbance at 505 nm was measured at 15-s intervals with 10 different concentrations of hydrogen peroxide standard solution (50, 100, 150, 200, 250, 300, 350, 400, 450, and 500 mg/l) and 1 blank solution. As shown in Fig. 1A, optical density (OD) of each solution increased with time; and the slope was directly related to the initial concentration of hydrogen peroxide. A calibration curve for the standard solution was developed by calculating slopes (absorbance increase at 505 nm/min × 1000) (Fig. 1B). The level of ROS was expressed using an arbitrary unit: one unit corresponds to 1 mg/l H_2O_2. The calibration curve for hydrogen peroxides was linear up to 500 units.

Detection limit of the method was obtained as four units from the analysis in Fig. 2: At this concentration, mean − 3(S.D.) of ROS level (2.19) was higher than mean + 3(S.D.) of the level (1.15) at zero.

Stability of measurement was demonstrated for two serum samples, which were diluted with various ratios: a simple linearity was observed between ROS levels and dilution ratios (Fig. 3).

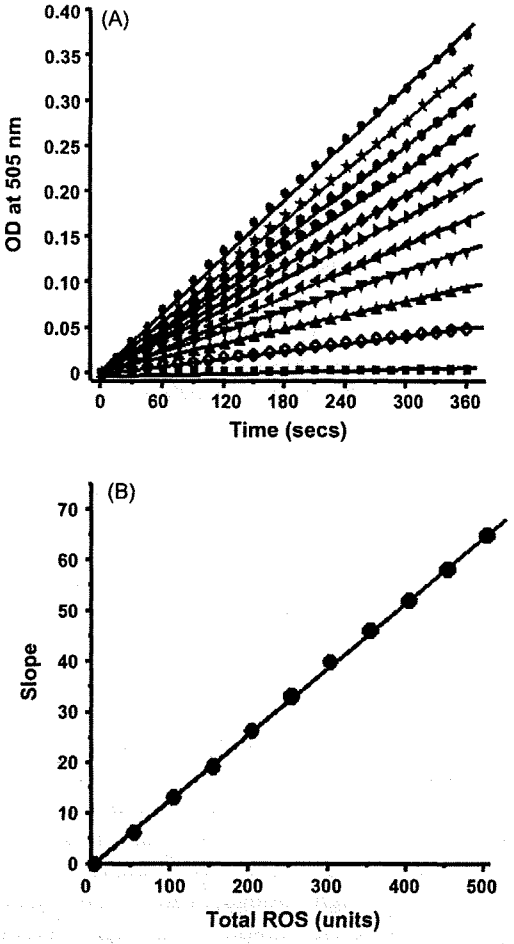

Fig. 1. Real-time measurement and calibration curve in the total ROS assay system. (A) Real-time measurement of seven different concentrations of standard sample ((■) blank, (○) 50, (▲) 100, (▼) 150, (◄) 200, (►) 250, (♦) 300, (⬟) 350, (⬢) 400, (⋆) 450, and (●) 500 units, respectively) and (B) calibration curve by hydrogen peroxide standard sample. Slope was calculated by [absorbance increase at 505 nm/min × 1000].

With regard to within-run reproducibility, serum samples with three different ROS levels were measured 12 times, resulting in very small coefficients of variation (CV), ranging from 2.4 to 2.7% (Table 1). The same samples were measured on five consecutive days for estimation of between-day reproducibility: CV ranged from 3.2 to 4.3% (Table 1).

The proposed assay system was applied to measure serum ROS levels, and the values of serum ROS were compared with those measured by the conventional D-ROM test. A good agreement in serum ROS levels among randomly selected 100 samples between these two methods was found in Fig. 4 with a high correlation coefficient of 0.94 ($P < 0.0001$).

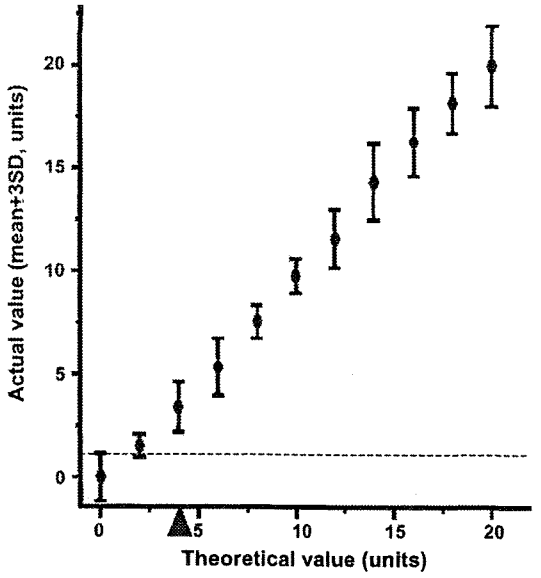

Fig. 2. Relation between actual and theoretical values of ROS. Bar indicates ± 3(S.D.). The dotted line indicates mean + 3(S.D.) at zero; (▲) indicates detection limit.

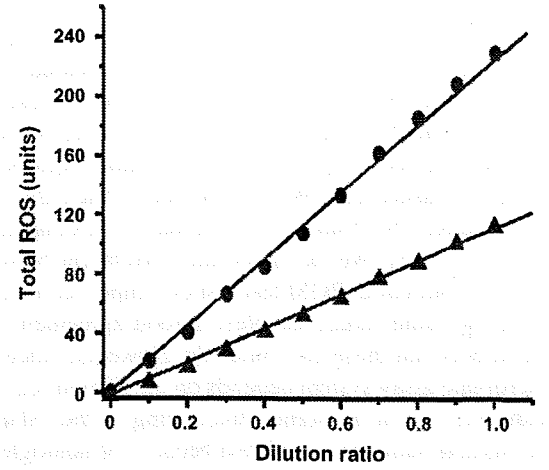

Fig. 3. Dilution linearity in the total ROS assay system. Serum samples from two healthy donors were diluted in a 10-phase process.

Table 1
Within-run and between-day precision

	Sample A	Sample B	Sample C
Within-run precision[a]			
Mean (units)	105.5	163.2	229.3
S.D.	2.7	1.5	5.4
CV (%)	2.5	2.7	2.4
Between-day precision[b]			
Mean (units)	100.0	161.1	225.1
S.D.	4.3	6.9	7.1
CV (%)	4.3	4.3	3.2

[a] Measured 12 times in a day.
[b] Measured at 5-day intervals.

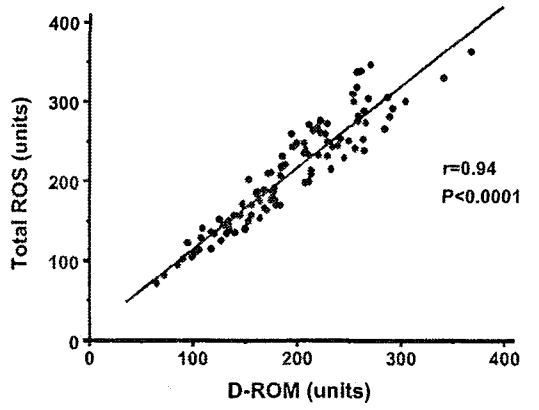

Fig. 4. Comparison of total ROS assay system with 96-well plate and D-ROM test performed using by FRAS (correlation coefficient 0.94, $P < 0.0001$, $n = 100$).

Next, the usefulness of this assay is demonstrated by way of example—assessing the effect of cigarette smoking on oxidative status in terms of serum ROS levels—since cigarette smoking is known to be the most potent factor relevant to increased oxidative stress in the body [23–28]. We measured serum ROS levels among 212 smokers and 40 never-smokers. The mean (±S.D.) ROS level among smokers, 211.6 ± 73.1 units was significantly higher than that among never-smokers (113.3 ± 24.0; $P < 0.0001$). Among smokers, serum ROS levels were found to increase with increased daily consumption of cigarettes (Fig. 5; $P < 0.0001$ for trend). In addition, the percentage increment of serum ROS level

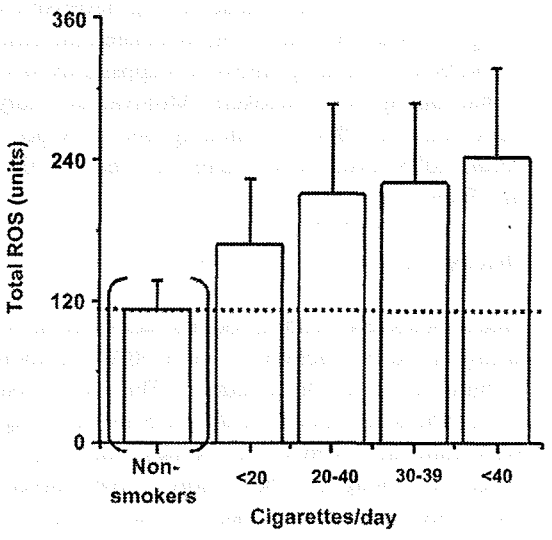

Fig. 5. Serum ROS levels by daily consumption of cigarettes. Examined were 40 never-smokers, and 35, 86, 56, and 35 current smokers with <20, 20–29, 30–39, and ≥40 cigarettes consumed per day, respectively. $P < 0.0001$ for trend.

Table 2
Percent increase of total ROS by age and smoking

Variables	Percent increment[a] (95% confidence interval)	β	P
Aging per 10-year	6.6 (2.5–10.7)	0.17	0.002
Cigarettes per pack per day	36.5 (28.6–44.9)	0.54	<0.0001

[a] Estimated by linear regression analysis.

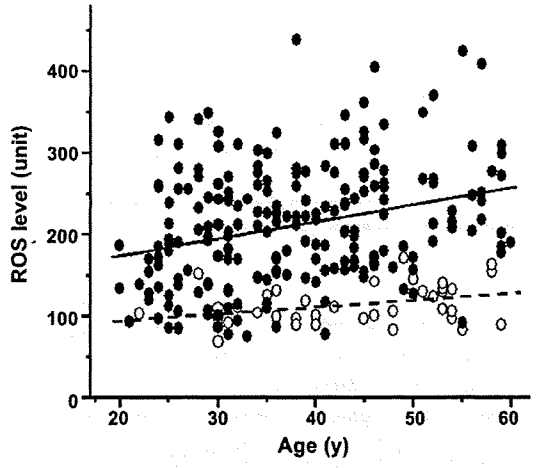

Fig. 6. Serum ROS levels by age and smoking status. Smokers (●) and never-smokers (○). Solid and dotted lines indicate regression lines for smokers and never-smokers, respectively.

per pack per day was 36.5% (95% confidence interval (CI), 28.6–44.9%; $P < 0.0001$), adjusting for age. Aging was also associated with increased serum ROS levels (6.6% increase/10-year, 95%CI: 2.5–10.7%; $P < 0.002$). It is evident in Fig. 6 that serum ROS levels among smokers were higher than those among never-smokers in all age groups, and that aging-associated increase of serum ROS levels among smokers is apparently steeper than that among never-smokers. Multivariate analysis revealed that the effect of smoking one pack per day on serum ROS levels was greater than that of 10-year aging (Table 2).

4. Discussion

Free radicals react with various molecules in the body, resulting in the production of stable ROS metabolites (e.g., lipid peroxide, DNA adduct). This assay system measured the total amount of the ROS in sera, a figure derived from various ROS metabolites formed recently and therefore thought to be a more stable marker for oxidative stress than other markers for momentary oxidative stress. Although the D-ROM test and microplate assay system for measurement of oxidative stress have been promoted as a useful approach for evaluation of ROS metabolites [10–15,19–21], clinical laboratories often require the routine measurement of ROS for a large number of serum samples, using a small sample volume and taking a shorter time. Thus, to improve its clinical usefulness, this automated assay system using a clinical chemical analyzer was developed. Here, we reported on a new assay system based upon modification of the conventional D-ROM test for automated measurements of ROS levels in serum. This new assay system can be performed with a conventional spectrophotometric plate reader according to kinetic analysis. Our data provided evidence that this assay system is a simple, reliable, high-throughput, and cost-effective method for the quantitative evaluation of oxidative stress, with acceptable stability and minimal imprecision. Specifically, this assay was shown to be applicable for measuring serum ROS levels of numerous samples with high reproducibility, requiring 5 min or less for measurement of 96 samples with 5 μl volume per sample. In contrast, the conventional D-ROM test takes 9 min or more for measurement of one sample with 20 μl volume required for a single measurement [9–15]. The microplate assay system requires 35–75 min for measurement of samples on a plate [19–21]. We examined the correlation between the conventional D-ROM test and our improved method using the same serum samples; a good agreement was found between these two methods. However, since the microplate assay system depends on the Fenton reaction with iron ions in the serum functioning as the catalyst, measurable samples are limited because of hemoglobin concentration in the serum [19–21]. Our method is different from the above method in that iron is added for enhancement of the Fenton reaction, absorbance can be automatically measured over time, and total ROS level can be measured from the slope of change in absorbance over time. Thus, this new system is superior in terms of simplicity and high-throughput, with no limitation in measurement samples due to hemoglobin concentration, compared with conventional systems. To summarize, the advantages of the newly developed system compared with the conventional one are shorter time consumed for the assay, smaller amounts of serum samples required for the assay, and an increased number of samples measured at once.

Cigarette smoke is known to increase production of oxygen free radicals by polymorph nuclear leukocytes

[29–31], and to decrease the activity levels of some free radical scavengers [32–35]. We found a significant correlation between serum ROS levels and daily consumption of cigarettes using this assay system. Thus, the assay system might enable us to estimate the deleterious effects of various risk factors of lifestyle-associated diseases on serum or plasma ROS levels among individuals, thereby contributing to risk estimates in epidemiology studies. We also anticipate that this assay will be useful as a surrogate biomarker in intervention studies to evaluate the efficacy of preventive measures, as well for clinical diagnosis of inflammation-associated diseases.

Acknowledgements

The Radiation Effects Research Foundation (RERF), Hiroshima and Nagasaki, Japan is a private, non-profit foundation funded by the Japanese Ministry of Health, Labour and Welfare (MHLW) and the U.S. Department of Energy (DOE) the latter through the National Academy of Sciences. This publication was supported by RERF Research Protocols RP# 1-93 and RP# 2-00 and in part by the Grant-in-Aid for Scientific Research from the Ministry of Education, Culture, Sports, Science, and Technology of Japan and for cancer research by the Ministry of Health and Welfare of Japan.

References

[1] B. Van Houten, V. Woshner, J.H. Santos, Role of mitochondrial DNA in toxic responses to oxidative stress, DNA Repair (Amst) 5 (2006) 145–152.
[2] F. Galli, M. Piroddi, C. Annetti, C. Aisa, E. Floridi, A. Floridi, Oxidative stress and reactive oxygen species, Contrib. Nephrol. 149 (2005) 240–260.
[3] J.K. Willcox, S.L. Ash, G.L. Catignani, Antioxidants and prevention of chronic disease, Crit. Rev. Food Sci. Nutr. 44 (2004) 275–295.
[4] E.G. Janzen, Y.L. Wang, Alpha-2,6-difluorophenyl-*N*-tert-butylnitrone: a spin trap for distinguishing different types of alkyl radicals based on long-range fluorine hyperfine splitting, Free Radic. Res. Commun. 10 (1990) 63–68.
[5] C.F. Babbs, D.W. Griffin, Scatchard analysis of methane sulfinic acid production from dimethyl sulfoxide: a method to quantify hydroxyl radical formation in physiologic systems, Free Radic. Biol. Med. 6 (1989) 493–503.
[6] J.C. Barreto, G.S. Smith, N.H. Strobel, P.A. McQuillin, T.A. Miller, Terephthalic acid: a dosimeter for the detection of hydroxyl radicals in vitro, Life Sci. 56 (1995) PL89–PL96.
[7] B. Halliwell, M. Grootveld, J.M. Gutteridge, Methods for the measurement of hydroxyl radicals in biomedical systems: deoxyribose degradation and aromatic hydroxylation, Methods Biochem. Anal. 33 (1988) 59–90.
[8] L. Parker (Ed.), Oxygen Radicals in Biological Systems, Academic Press, New York, 1994.
[9] A. Aberti, L. Bolognini, M. Carratelli, M.A. Della Bona, D. Mavviantelli, Assessing oxidative stress with the D-Roms test. Some mechanistic consideration, in: Proceedings of the SFRR Summer Meeting, 1997, pp. 82–83.
[10] M.R. Cesarone, G. Belcaro, M. Carratelli, U. Cornelli, M.T. De Sanctis, L. Incandela, A. Barsotti, R. Terranova, A. Nicolaides, A simple test to monitor oxidative stress, Int. Angiol. 18 (1999) 127–130.
[11] A. Alberti, L. Bolognini, D. Macciantelli, M. Cratelli, The radical cation of *N,N*-diethyl-*para*-phenylendiamine: a possible indicator of oxidative stress in biological samples, Res. Chem. Intermed. 26 (2000) 253–267.
[12] R. Trotti, M. Carratelli, M. Barbieri, G. Micieli, D. Bosone, M. Rondanelli, P. Bo, Oxidative stress and a thrombophilic condition in alcoholics without severe liver disease, Haematologica 86 (2001) 85–91.
[13] U. Cornelli, R. Terranova, S. Luca, M. Cornelli, A. Alberti, Bioavailability and antioxidant activity of some food supplements in men and women using the D-Roms test as a marker of oxidative stress, J. Nutr. 131 (2001) 3208–3211.
[14] M. Carratelli, L. Porcaro, M. Ruscica, E. De Simone, A.A. Bertelli, M.M. Corsi, Reactive oxygen metabolites and prooxidant status in children with Down's syndrome, Int. J. Clin. Pharmacol. Res. 21 (2001) 79–84.
[15] R. Trotti, M. Carratelli, M. Barbieri, Performance and clinical application of a new, fast method for the detection of hydroperoxides in serum, Panminerva Med. 44 (2002) 37–40.
[16] G. Mantovani, A. Maccio, C. Madeddu, L. Mura, G. Gramignano, M.R. Lusso, V. Murgia, P. Camboni, L. Ferreli, M. Mocci, E. Massa, The impact of different antioxidant agents alone or in combination on reactive oxygen species, antioxidant enzymes and cytokines in a series of advanced cancer patients at different sites: correlation with disease progression, Free Radic. Res. 37 (2003) 213–223.
[17] S. Salardi, S. Zucchini, D. Elleri, G. Grossi, A.M. Bargossi, S. Gualandi, R. Santoni, A. Cicognani, E. Cacciari, High glucose levels induce an increase in membrane antioxidants, in terms of vitamin E and coenzyme Q10, in children and adolescents with type 1 diabetes, Diabetes Care 27 (2004) 630–631.
[18] C. Vassalle, C. Boni, P. Di Cecco, P. Landi, Elevated hydroperoxide levels as a prognostic predictor of mortality in a cohort of patients with cardiovascular disease, Int. J. Cardiol. 110 (2006) 415–416.
[19] G. Brambilla, M. Fiori, L.I. Archetti, Evaluation of the oxidative stress in growing pigs by microplate assays, J. Vet. Med. A Physiol. Pathol. Clin. Med. 48 (2001) 33–38.
[20] G. Brambilla, C. Civitareale, A. Ballerini, M. Fiori, M. Amadori, L.I. Archetti, M. Regini, M. Betti, Response to oxidative stress as a welfare parameter in swine, Redox Rep. 7 (2002) 159–163.
[21] A. Ballerini, C. Civitareale, M. Fiori, M. Regini, M. Betti, G. Brambilla, Traceability of inbred and crossbred Cinta Senese pigs by evaluating the oxidative stress, J. Vet. Med. A Physiol. Pathol. Clin. Med. 50 (2003) 113–116.
[22] M. Nakamura, Study on establishment of smoking cessation methods for primary prevention of smoking-related cancer, Report by FY1998 MHLW grant-in aid for cancer, 1998, 639–641 (Japanese).
[23] C.S. Liu, H.W. Chen, C.K. Lii, S.C. Chen, Y.H. Wei, Alterations of small-molecular-weight antioxidants in the blood of smokers, Chem. Biol. Interact. 116 (1998) 143–154.
[24] S. Loft, H.E. Poulsen, Cancer risk and oxidative DNA damage in man, J. Mol. Med. 74 (1996) 297–312.

[25] A.R. Puhakka, T.H. Harju, P.K. Paakko, Y.M. Soini, V.L. Kinnula, Nitric oxide synthases are associated with bronchial dysplasia, Lung Cancer 51 (2006) 275–282.
[26] R.A. Saleh, A. Agarwal, R.K. Sharma, D.R. Nelson, A.J. Thomas Jr., Effect of cigarette smoking on levels of seminal oxidative stress in infertile men: a prospective study, Fertil. Steril. 78 (2002) 491–499.
[27] M.G. Traber, A. van der Vliet, A.Z. Reznick, C.E. Cross, Tobacco-related diseases. Is there a role for antioxidant micronutrient supplementation? Clin. Chest. Med. 21 (2000) 173–187.
[28] V.L. van Antwerpen, A.J. Theron, G.A. Richards, K.J. Steenkamp, C.A. van der Merwe, R. van der Walt, R. Anderson, Vitamin E, pulmonary functions, and phagocyte-mediated oxidative stress in smokers and nonsmokers, Free Radic. Biol. Med. 18 (1995) 935–941.
[29] R. Ross, The pathogenesis of atherosclerosis—an update, N. Engl. J. Med. 314 (1986) 488–500.
[30] P. Maity, K. Biswas, S. Roy, R.K. Banerjee, U. Bandyopadhyay, Smoking and the pathogenesis of gastroduodenal ulcer—recent mechanistic update, Mol. Cell. Biochem. 253 (2003) 329–338.
[31] J.S. Dunn, B.M. Freed, D.L. Gustafson, K.A. Stringer, Inhibition of human neutrophil reactive oxygen species production and p67phox translocation by cigarette smoke extract, Atherosclerosis 179 (2005) 261–267.
[32] W.A. Pryor, D.F. Church, C.K. Govindam, G. Vrank, Oxidation of thiols by nitric oxide and nitrogen dioxide: synthetic utility and toxicological implication, J. Org. Chem. 47 (1982) 156–159.
[33] L. Guemouri, Y. Artur, B. Herbeth, C. Jeandel, G. Cuny, G. Siest, Biological variability of superoxide dismutase, glutathione peroxidase, and catalase in blood, Clin. Chem. 37 (1991) 1932–1937.
[34] E. Nishio, Y. Watanabe, Cigarette smoke extract is a modulator of mitogenic action in vascular smooth muscle cells, Life Sci. 62 (1998) 1339–1347.
[35] M. Unlu, F. Fidan, M. Sezer, L. Tetik, O. Sahin, H. Esme, T. Koken, M. Serteser, Effects of melatonin on the oxidant/antioxidant status and lung histopathology in rabbits exposed to cigarette smoke, Respirology 11 (2006) 422–428.

Available online at www.sciencedirect.com
ScienceDirect
Journal of Steroid Biochemistry & Molecular Biology 105 (2007) 106–114
The Journal of Steroid Biochemistry & Molecular Biology
www.elsevier.com/locate/jsbmb

Demethylation of promoter C region of estrogen receptor α gene is correlated with its enhanced expression in estrogen-ablation resistant MCF-7 cells

Tetsuya Sogon[a,b], Shigeru Masamura[c], Shin-ichi Hayashi[d], Richard J. Santen[e], Kei Nakachi[a,b], Hidetaka Eguchi[a,b,*]

[a] *Department of Molecular Epidemiology, Hiroshima University Graduate School of Biomedical Sciences, Radiation Effects Research Foundation, 5-2, Hijiyama-park, Minami-ku, Hiroshima 732-0815, Japan*
[b] *Department of Radiobiology/Molecular Epidemiology, Radiation Effects Research Foundation, 5-2, Hijiyama-park, Minami-ku, Hiroshima 732-0815, Japan*
[c] *Department of Surgery, Tokyo Dental College Ichikawa General Hospital, 5-11-13, Sugano, Ichikawa, Chiba 272-8513, Japan*
[d] *Department of Medical Technology, Tohoku University School of Medicine, 2-1, Seiryocho, Aoba-ku, Sendai 980-8575, Japan*
[e] *University of Virginia Health System, Charlottesville, VA 22908, USA*

Received 7 July 2006; accepted 29 December 2006

Abstract

Long-term estrogen deprivation (LTED) MCF-7 cells showing estrogen-independent growth, express estrogen receptor (ER) α at a much higher level than wild-type MCF-7 cells. Enhanced expression of ERα associated with partial localization of ERα to the plasma membranes in LTED cells is thought to be an important step for acquisition of estrogen-ablation resistance. In this study, we compared the regulation of ERα gene expression between wild type and LTED cells, examining the usage of the promoters A and C as well as their methylation status. We found that transcription from the promoter C was drastically enhanced in LTED cells, compared with that in wild-type cells. Furthermore, the promoter C region was highly unmethylated in LTED cells, but partially methylated in wild-type cells. Our findings imply that demethylation of promoter C region in the ERα gene is in part responsible for the enhanced expression of ERα gene in LTED cells.

Keywords: Estrogen receptor α; Breast cancer; Methylation

1. Introduction

Experimental, clinical, and epidemiologic data suggest that estrogens contribute to the development of breast cancer. Estrogens bind to ERα or β and stimulate the transcription of target genes involved in cell proliferation. Thus, the anti-estrogen therapy such as tamoxifen has been generally used for ERα-positive breast cancer for several decades. Recently, clinical trials in the adjuvant, neoadjuvant and advanced disease setting have demonstrated a greater clinical efficacy of the aromatase inhibitors aiming to decrease the concentration of estrogen, compared with selective estrogen receptor modulators represented by tamoxifen [1,2]. On the other hand, clinical observations suggested that some human breast cancers adapted to hormone-ablative therapy involving surgically deprivation of estrogen production. Hormone-dependent breast cancers often regress in response to surgical removal of the ovaries, a treatment which lower circulating plasma estradiol (E2) from approximately 200–15 pg/ml [3]. In response to this acute deprivation of E2, tumors regress for 12–18 months on average before they begin to regrow. Second-line therapy with surgical oophorectomy or with aromatase inhibitors can then induce additional tumor regression by lowering E2 concentrations further to 1–5 pg/ml [4]. These

* Corresponding author at: Department of Radiobiology/Molecular Epidemiology, Radiation Effects Research Foundation, 5-2, Hijiyama-park, Minami-ku, Hiroshima 732-0815, Japan. Tel.: +81 82 261 3169; fax: +81 82 261 3170.
E-mail address: eguchi@rerf.or.jp (H. Eguchi).

0960-0760/$ – see front matter © 2007 Elsevier Ltd. All rights reserved.
doi:10.1016/j.jsbmb.2006.12.104

observations for the first time demonstrated enhanced sensitivity to circulating E2.

In order to demonstrate the phenomenon of adaptive hypersensitivity and to determine the mechanisms involved, we have established a model system involving MCF-7 human breast cancer cells *in vitro*. Wild-type MCF-7 cells were cultured over a prolonged period in estrogen-free medium to mimic the effect of ablative endocrine therapy such as induced by surgical oophorectomy [5]. This process involves long-term E2 deprivation; the adapted cells are called LTED cells. When LTED cells were cultured in the presence of E2 for 4 months, the cells showed estrogen-dependent growth as was observed for wild-type MCF-7 cells [5].

Importantly, ERα is expressed at a much higher level in LTED cells than in wild-type MCF-7 cells [6]. In concert with this observation, an elevated basal ER transactivation activity (mean increase; 5-fold) was measured in LTED cells compared with the wild-type cells using pERE-tk-CAT, a reporter gene driven by estrogen responsive element-thymidine kinase promoter [6].

In addition to the established role as a nuclear receptor, ERα may have another function on the plasma membrane. In LTED cells, ERα localizes predominantly to the nuclei and some also present on the plasma membranes [7]. The sub-cellular localization of ERα to the plasma membranes in LTED cells may, at least in part, be due to the enhanced expression of ERα in LTED cells, since plasma membrane-associated ERα can only be observed in ERα-enriched MCF-7 sub-cell lines (mER^{high}) but not ERα-depleted ones ($mER\alpha^{low}$) [8]. Constitutively activated MAP kinase activity was observed in LTED cells independent of serum factors [9]. A rapid physical interaction of the plasma membrane-associated ERα and an adaptor protein Shc has been observed upon addition of E2 [7]; Shc is subsequently phosphorylated and triggers the MAP kinase signaling pathway [10,11].

Thus, when ERα works as a transcription factor in the nuclei and also as a signal transducer on the plasma membranes, typically in LTED cells, enhanced expression of ERα may be an obligatory step for acquisition of estrogen-ablation resistance. Though, the mechanisms how ERα expresses at high level in LTED cells still remain unknown.

Several human ERα gene promoters (A–F) are identified so far [12]. These promoters are differently utilized in a tissue- and cell-dependent manner [13–15]. Among these promoters, we previously demonstrated that the transcript from promoter A was constitutively used in both normal and cancerous mammary tissue, while the transcript from promoter C (formerly called promoter B) showed remarkable correlation to the ERα protein levels in ERα-positive breast cancer [16]. Furthermore, we have identified a *cis*-acting element, ERBF-1, that plays an important role in the expression of the ERα gene transcribed from promoter C in breast cancer cells [17]. On the other hand, a transcription factor ERF-1, a member of AP2 transcription factor, is important for the transcriptional regulation of promoter A [18,19]. In addition, methylation of the promoter A and C regions was critical for the repression of gene transcription from these promoters [20]. Collectively, methylation of these promoter regions as well as alteration of critical transcription factors are thought to be important for ERα gene expression in breast cancer cells.

In this study, we examined regulation of ERα gene expression in wild-type MCF-7 and LTED cells. We first found that transcription from the promoter C was drastically enhanced in LTED cells, compared with that in the wild-type cells. Transient transfection with a reporter gene driven by the promoter A or promoter C of ERα gene revealed that transcription factors are equally available in these cells. Second, differences in epigenetic alterations of promoter C were found between LTED and wild-type cells: The promoter C region was highly unmethylated in LTED cells, while that in wild-type cells was partially methylated. Our findings imply that demethylation of promoter C region in the ERα gene is in part responsible for the enhanced expression of ERα gene in LTED cells.

2. Materials and methods

2.1. Tissue culture

Human breast cancer cells wild-type MCF-7 were maintained in improved MEM (IMEM) containing 5% dextran-coated charcoal-stripped fetal bovine serum (DCC-FBS) and 10 nM E2. LTED cells were established by long-term culture of wild-type MCF-7 cells in IMEM containing 5% DCC-FBS. The established LTED cells were stored in liquid nitrogen until use. LTED cells were maintained in IMEM containing 5% DCC-FBS.

2.2. Plasmid

Reporter plasmids pGL3-ProA 1.3K and pGL3-ProC (formerly called pGL3-ProB1.4K) were described previously [20]. An internal control pRL-TK was purchased from Promega (Madison, WI).

2.3. RNA extraction and cDNA synthesis

Total RNA was prepared from wild type and LTED cells using RNeasy Mini kit (QIAGEN, Hilden, Germany). One μg of total RNA was reverse transcribed with Quantitect Reverse Transcription (QIAGEN) using RT primer mix as primers in a final volume of 20 μl at 42 °C for 15 min.

2.4. Real-time PCR analysis of ERα mRNA expression

The real-time PCR was performed in triplicate using iCycler iQ (Bio-Rad Laboratories, Hercules, CA). Reaction mixture consisted of 1 μl of cDNA products, 0.2 μM of each primers and 12.5 μl of SYBR Green ROX Mix (ABgene, Epsom, UK) in a total volume of 25 μl. PCR thermal conditions were as following: 95 °C for 15 min for 1 cycle and 95 °C for 20 s, 60 °C for 15 s, 72 °C for 10 s, and 86 °C for

15 s (fluorescent signal collection) for 50 cycles for detection of ERα mRNA from promoters A and C; 95 °C for 15 min for 1 cycle and 94 °C for 15 s, 68 °C for 30 s, and 86 °C for 15 s (fluorescent signal collection) for 50 cycles for detection of total ERα mRNA. The following primers were used: PROA1, 5′-ACC TCG GGC TGT GCT CTT-3′ and PRODW, 5′-GAG GGT CAT GGT CAT GGT-3′ for ERα mRNA from promoter A; PROB3, 5′-GCC CAG GAA CAT TTC TGG AA-3′ and PRODW for ERα mRNA from promoter C; EREX1, 5′-AGA ACG AGC CCA GCG GCT AC-3′ and EREX2-R, 5′-CCT TGC AGC CCT CAC AGG AC-3′ for total ERα mRNA. For construction of standard curves, serially diluted plasmids harboring fragment of target gene sequences were used after digestion with *Not* I restriction enzyme to release the insert fragments. As a control, β-actin mRNA was also measured as described previously [21].

2.5. Transient transfection assays

A transient transfection of the plasmids was performed in triplicate using SuperFect Transfection Reagent (QIAGEN) under manufacturer's instruction. Briefly, 1×10^5 cells were plated onto 24 wells plastic dish. After over night culture, 1 μg of pGL3-ProA1.3K or pGL3-ProC and 0.1 μg of pRL-TK were mixed with 5 μl of the SuperFect Transfection Reagent in 350 μl of the medium with 5% DCC-FBS and subjected to transfection. After 2 h incubation, the medium was replaced with a fresh medium and cells were incubated for 48 h. Then, cells were collected and lysed using Passive Lysis Buffer (Promega). Luciferase assays were performed using Dual-Luciferase Reporter Assay System (Promega) and TD-20/20 Luminometer (TURNER DESIGNS, CA).

2.6. Bisulfite modification and methylation-specific PCR

Total DNA was extracted from wild type and LTED cells using NucleoSpin Tissue (MACHEREY-NAGEL, Düren, Germany). DNA was subjected to bisulfite conversion using EZ DNA Methylation kit (ZYMO Research, Orange, CA) according to the manufacture's instruction, essentially based on the report by Herman et al. [22]. Briefly, after denaturation with NaOH, 500 ng of DNA was incubated in a buffer containing sodium bisulfite at 50 °C for 16 h, followed by purification using ZYMO-Spin I column. Bisulfite-converted DNA was eluted in 10 μl of M-Elution buffer. First PCR amplification aiming to amplify bisulfite-converted DNA fragments was performed in 20 μl of reaction mixture containing 1 μl of bisulfite-treated genomic DNA, 0.5 μM each primers, 0.2 mM dNTPs, 2.5 mM $MgCl_2$ and 1.25 units of AmpliTaq Gold DNA polymerase (Applied Biosystem, Foster, CA) under the following conditions: 95 °C for 5 min for 1 cycle and 95 °C for 15 s, 54 °C for 15 s, and 72 °C for 1 min for 35 cycles. Second PCR amplification using methylation- or unmethylation-specific primers was performed in 20 μl of reaction mixture containing 1 μl of first PCR product (1/100 diluted with MilliQ water), 0.5 μM each primers, 0.2 mM dNTPs, 2.5 mM $MgCl_2$ and 1.25 units of AmpliTaq Gold DNA polymerase under the following conditions: 95 °C for 5 min for 1 cycle and 95 °C for 15 s, 57 °C (methylation) or 54 °C (unmethylation) for 30 s, and 72 °C for 20 s for 35 cycles. The amplified fragments were electrophoresed to 8% polyacrylamide gel. All the primers used for this methylation analysis were designed using MethPrimer [23]. Primers used for the first PCR and second PCR are summarized in Table 1.

For quantification, real-time PCR amplification was performed in 25 μl of reaction mixture containing 1 μl of the first PCR product (1/100 diluted with MilliQ water), 0.2 μM each primers and 12.5 μl of SYBR Green Rox Mix according to the manufacturer's protocol using iCycler iQ under the following conditions: 95 °C for 15 min for 1 cycle and 95 °C for 15 s, 57 °C (methyl) or 54 °C (unmethyl) for 15 s, 72 °C for 15 s, and fluorescent signal collection at 77 °C (methyl) or 76 °C (unmethyl) for 20 s for 40 cycles. The assay was conducted in triplicate and repeated for three times. For construction of a standard curve, serially diluted control PCR fragments were used.

Table 1
Primers used for the methylation-specific PCR

Promoter	PCR	Specification	Primer name	Primer sequence	Annealing temperature (°C)
A	1st	Bisulfite conversion specific	ERPROABSF	5′-TTAATGTTAGGGTAAGGTAATAGTTTT-3′	54
			ERPROABSR	5′-AACCACCTAAAAAAAAAACACAA-3′	
	2nd	Methylation specific	ERPROAM1F	5′-AGTTTAGGAGTTGGCGGAGGGC-3′	60
			ERPROAM1R	5′-CCGAAATTAAAAACGACGCAACG-3′	
		Unmethylation specific	ERPROAU1F	5′-GGGAGTTTAGGAGTTGGTGGAGGGT-3′	60
			ERPROAU1R	5′-ACCCAAAATTAAAAACAACACAACACA-3′	
C	1st	Bisulfite conversion specific	ERPROCBSF	5′-AGTAGATAGTAAGTTTTTTTTTATTTTTT-3′	54
			ERPROCBSR	5′-AAAAACAACCAATAAACAAAA-3′	
	2nd	Methylation specific	ERPROCM1F	5′-TTTTTTATTGTTATTTATTTAGCGT-3′	57
			ERPROCM1R	5′-AAAACACTTAACAACCCCTCCCGAC-3′	
		Unmethylation specific	ERPROCU1F	5′-TATTTTTTATTGTTATTTATTTAGTGT-3′	54
			ERPROCU1R	5′-AAACACTTAACAACCCCTCCCAAC-3′	

2.7. Bisulfite-sequencing and combined bisulfite restriction analysis (COBRA)

PCR amplification of ERα promoter C region using bisulfite-converted DNA fragments was performed as described above except for the cycle numbers to be 50. The amplified fragments were purified using NucleoSpin Extract II kit (MACHEREY-NAGEL). Direct sequencing of the fragments was conducted using ERPROCBSF as a primer, BigDye Terminators v1.1 Cycle Sequencing Kit and ABI PRISM 310 Genetic Analyzer (Applied Biosystems, Foster City, CA). For COBRA, 5 μl of purified DNA fragment was digested in a total volume of 20 μl using 5 units of *Hpy*188III restriction enzyme (New England BioLabs, Ipswich, MA) that cleave CpG sites retained because of methylation at 37 °C for 4 h. The resultant DNA fragments together with undigested ones were electrophoresed onto 8% polyacrylamide gel. After staining with ethidium bromide, the image was visualized under UV illumination. Intensity of the fluorescence of each band was quantified using ChemImager 5500 (Alpha Innotech, San Leandro, CA).

2.8. Statistical analysis

Student's *t*-test was conducted for statistical analysis. When necessary, the *t*-test was modified to all for unequal variances. *P*-values less than 0.05 were considered as significant.

3. Results

3.1. Expression levels of ERα mRNA in wild-type and LTED cells

We previously demonstrated that ERα protein and mRNA were expressed at higher levels in LTED cells than in wild-type cells using Western and Northern blot analyses [6]. As a first step, we conducted real-time PCR analysis to quantitatively evaluate ERα mRNA expression in wild-type and LTED cells: LTED cells showed 27-fold total ERα mRNA expression levels as compared with wild-type cells did ($P = 0.004$) (Fig. 1).

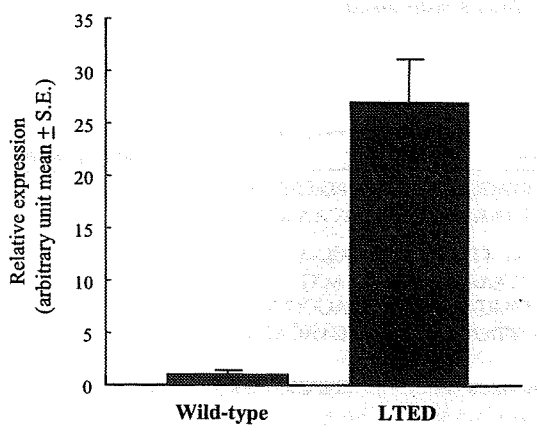

Fig. 1. Relative expression of total ERα mRNA in wild type and LTED cells. Real-time RT-PCR was conducted for quantification of total ERα and β-actin mRNA as described in Section 2. Expression levels of total ERα mRNA were normalized using β-actin mRNA.

Since an increase of ERα mRNA from promoter C was responsible for the enhanced expression of ERα protein in ERα-positive primary breast cancer and since promoter A was constitutively utilized in both normal and cancerous mammary tissue [16], we next compared ERα mRNA expression levels transcribed from these promoters A and C between wild-type and LTED cells using real-time PCR (Fig. 2). ERα mRNA from promoter A in LTED cells was 35-fold higher than that in wild-type cells ($P = 0.0007$) (Fig. 2). Furthermore, ERα mRNA expression level from promoter C in LTED was 149-fold higher than that in wild-type cells ($P = 0.01$) (Fig. 2). In wild-type cells, promoter A was dominant while promoters A and C were equally utilized in LTED cells (Fig. 2). These results indicate that reinforced utilization of promoter C in LTED cells as compared with wild-type cells may be important for the enhanced expression of ERα in LTED cells.

3.2. Transient transfection of reporter gene constructs with ERα gene promoters

The *cis*- and *trans*-acting factors are thought to generate differences in transcription activity on various promoters. We first tested the possibility that alterations of transcription factors may generate an increased level of ERα expression in LTED cells, compared with wild-type cells. We then measured the promoter activities in wild type and LTED cells using reporter gene constructs driven by ERα promoters A and C. No significant differences in promoter activities between wild-type and LTED cells were observed for these two promoters ($P = 0.3$ and 0.1 for promoters A and C, respectively, Fig. 3), suggesting that *trans*-acting factors specific to promoters A and C are not responsible for the different utilization of ERα promoters A and C between wild-type and LTED cells.

3.3. Different methylation status of ERα gene promoters in wild-type and LTED cells

We next hypothesized that alternations of higher order chromatin structure caused by DNA methylation may contribute to the expression level of ERα in these cells. Then, we compared methylation status of ERα gene promoters A and C in wild-type and LTED cells by methylation-specific PCR. Promoter A of ERα gene was unmethylated in both wild-type and LTED cells (Fig. 4). On the other hand, promoter C of ERα gene showed partial methylation in wild-type cells (Fig. 4), in good agreement with our previous report [20]. In LTED cells, the unmethylated band for promoter C was clearly observed, while the methylated one was considerably weaker (Fig. 4), in accordance with our